Organic Electronics 82 (2020) 105737

Contents lists available at ScienceDirect

Organic Electronics

journal homepage: http://www.elsevier.com/locate/orgel

Efficient and stable mesoporous perovskite solar cells using p-type poly (9-vinylcarbazole) modified the interface of perovskite/mesoporous TiO_2 layers

Jiaji Duan [a], Yuning Liu [a], Xiaohong Chen [a,*], Sumei Huang [a], Wei Ou-Yang [a], Guang Zhu [c,**], Sanjun Zhang [b,d], Zhuo Sun [a]

[a] Engineering Research Center for Nanophotonics & Advanced Instrument, Ministry of Education, School of Physics and Electronic Science, East China Normal University, Shanghai, 200241, PR China
[b] State Key Laboratory of Precision Spectroscopy, East China Normal University, 3663 North Zhongshan Road, Shanghai, 200062, PR China
[c] Key Laboratory of Spin Electron and Nanomaterials of Anhui Higher Education Institutes, Suzhou University, Suzhou, 234000, PR China
[d] Collaborative Innovation Center of Extreme Optics, Shanxi University, Taiyuan, Shanxi, 030006, PR China

ARTICLE INFO

Keywords:
Perovskite solar cell
Stability
Interface modification
TiO_2
poly(9-vinylcarbazole)

ABSTRACT

A p-type poly(9-vinylcarbazole) (PVC) was inserted into the interface between perovskite and mesoporous TiO_2 electron transport layers. The ultrathin PVC modified TiO_2 layer can obviously improve the crystallinity of perovskite layer with less pinholes, passivate the interface and inhibit hole carriers transport into the interface of perovskite/TiO_2 electron transport layers. The perovskite film modified with PVC shows larger grain sizes and more compact films, which helps to increase photocurrent and reduce the leak current of cells. The passivating interface with less hole carrier accumulation and hydrophobicity can greatly reduce carrier recombination, improve carrier transport and extraction abilities and cells stability. Therefore, perovskite solar cells (PSCs) with PVC modified TiO_2 layer exhibited a power conversion efficiency (PCE) of 19.02%, which is remarkably higher than that (16.09%) of the reference cells. Furthermore, PSCs without and with PVC modification respectively retained 20% and 55% of the initial PCE values aging for 30 days at the relative humidity 15% in air without encapsulation. For thermal stability test, the pervoskite layers were heated for 10 h at 100 °C before further spin-coating Spiro-OMeTAD, PSCs with PVC modification were still remained 70% of the original PCEs, which is greatly higher than that (30%) of the reference cells. These results indicate that PSCs with PVC modified TiO_2 layer can effectively improve PCEs and show better moisture resistance and thermal stability.

1. Introduction

Perovskite solar cells (PSCs) with organometal halides have recently emerged as a prominent, efficient and low-cost solar technology. The power conversion efficiencies (PCEs) of mesoporous PSCs have exceeded 24.2% [1–4]. In the typical mesoporous PSC configuration, the perovskite photoactive layer is normally sandwiched with compacting/mesoporous TiO_2 electron transport layers (ETLs) and the hole transport layer to transport and collect carriers produced from perovskite layer [5–9]. The transport distance of electrons compared to holes in $MAPbI_3$ perovskite layer is significantly shorter [6]. Therefore, the exploration of the novel electron transport materials for mesoporous PSCs is always an interesting and important scientific challenge, including synthetic methodology for an appropriate energy level alignment along with perovskite layer [8] Many metal oxides such as zinc oxide (ZnO) [10], tin oxide (SnO_2) [11,12] and titanium dioxide (TiO_2) [13,14] have been applied as electron transport layers (ETLs) for solar cells. Among these metal oxides, TiO_2 is still a good ETL material due to its chemical stability, low cost, and the matched band energy level with the perovskite layer.

TiO_2 as a compacting and mesoporous electron transport layer has extensively investigated and still got the best PCEs among all kinds of PSCs. However, there are still larger room to improve the performance of mesoporous PSCs based on TiO_2 layer [15–17]. Some typical

* Corresponding author.
** Corresponding author.
E-mail addresses: xhchen@phy.ecnu.edu.cn (X. Chen), guangzhu@ahszu.edu.cn (G. Zhu).

https://doi.org/10.1016/j.orgel.2020.105737
Received 15 November 2019; Received in revised form 18 January 2020; Accepted 13 March 2020
Available online 25 March 2020

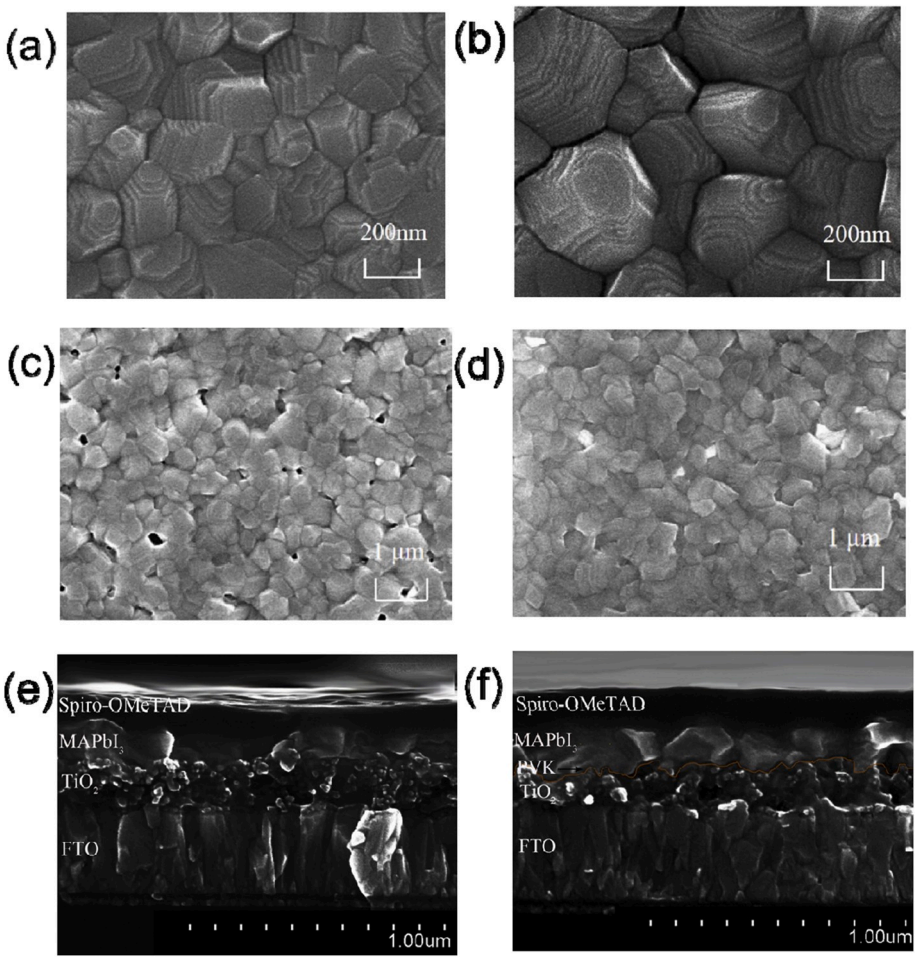

Fig. 1. Top view SEM images of perovskite films grown on pure TiO_2 layers (a, c) and PVC modified TiO2 layers (b, d). Cross-sectional SEM images of PSCs without (e) and with (f) PVC modification. The PVC concentration of the modified TiO_2 layer is 1 mg ml^{-1}.

problems such as reducing photo-oxidation and pinholes of the perovskite layer, improving contact properties and inhibiting carrier recombination still need further be solved to improve the performance of PSCs, especially stability. The dopant ions such as Li^+, Mg^+, Sn^+ doping TiO_2 layers have been demonstrated an efficient method to improve the conductivity of TiO_2 layer and reduce the trap states of interfaces of PSCs [18–20]. The interface modification by introducing inorganic materials such as chlorine-capped TiO_2 nanoparticles can enhance the performance of cells due to defect passivation of the interface between perovskite and ETLs [18]. The organic material such as $PC_{61}BM$, $PC_{71}BM$ [21], PMMA [22] modified TiO_2 have been suggested which can help to improve the crystallization of perovskite and contact properties, leading to greatly improving the performance of PSCs.

However, the p-type organic materials modified TiO_2 mesoporous/compacting electron transport layers show few reports to improve the performance of PSCs. As a widely used p-type semiconducting polymer, poly(9-vinylcarbazole) (PVC) can effectively transport hole carriers in photorefractive applications [23,24] and organic solar cells [25]. The N atoms of PVC can form hydrogen bonds with a hydroxyl proton of TiO_2 surface and I^- ions of perovskite and further interact with Pb^{2+} ions of perovskite [26–29]. Considering that PVC is a wide band-gap material with the advantages of hydrophobicity and interaction between N atoms of PVC and TiOx/perovskite interface, using PVC as a modified layer is expected to improve crystallization of perovskite layer and contact properties, passivate the defects, and inhibit hole carriers to transport into the interface of TiO_2/perovskite layers. Therefore, compared to interface modification of n-type organic materials, the p-type PVC with the wide band gap modified TiO_2 ETLs have more advantages for reducing holes accumulation and carrier recombination at the interface of TiO_2/perovskite layers. PSCs with PVC modified TiO_2 ETLs showed higher PCEs and better stability, indicating that p-type organic materials modified TiO_2 electron transport layer is an effective method to improve the performance of PSCs.

2. Experimental

2.1. Materials

Tetra-n-butyl titanate $Ti(OC_4H_9)_4$, methanol and ethanol were purchased from Sinopharm Chemical Reagent Co. Ltd. China. TiO_2 paste (Dyesol 18-NRT) was purchased from Dyesol Company. Γ-butyrolactone (GBL), dimethylsulfoxide(DMSO), Lithiubis(trifluoromethanesulfonyl) imide (Li-TFSI, 98%) and 4-tert-butylpyridine (TBP, 98%) were purchased from Aladdin company (Shanghai, China). Lead (II) iodide (PbI_2, 99.999%) and ethyl cellulose were purchased from Sigma-Aldrich. CH_3NH_3I (MAI) was purchased from 1-Material-Organic Nano Electronic (1-Material Inc.). 2,2′,7,7′-tetrakis (N,N-di-p-methoxy-phenylamine)-9,9′-spirobifluorene (Spiro-OMeTAD, ≥99%) was purchased from Polymer Light Technology Corp. (Xi'an, China). Poly(9-vinylcarbazole) (PVC) was purchased from Acros organics (USA).

2.2. Device fabrication

The patterned FTO with 14 Ω/cm^2 substrates were ultrasonically

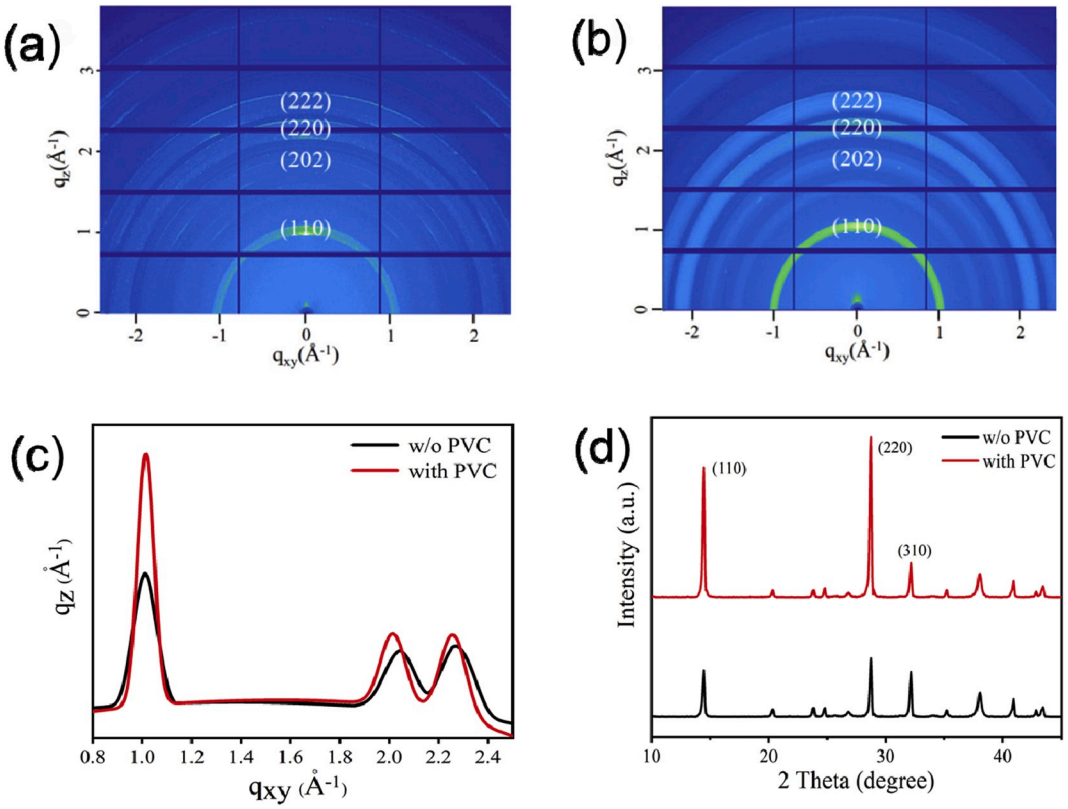

Fig. 2. GIWAXS images of perovskite films modified without (a) and with (b) PVC. (c) In-plane lines integrated from corresponding 2D GIWAXS patterns. (d) XRD patterns of perovskite films.

cleaned using deionized water, acetone and isopropanol, then blow dried with nitrogen gas and then treated under UV-ozone for 15 min to remove the organic residue. A precursor solution fabricating the compact TiO_2 layer was blended from isopropyl titanate and ethanol (222 μL:5 mL). The compact TiO_2 layer was spin-coated onto FTO substrate at 4000 rpm for 30 s and then sintered at 500 °C for 30 min. The mesoporous TiO_2 films were deposited on the compact TiO_2 layer by spin-coating TiO_2 paste diluted in anhydrous ethanol (weight ratio: 1: 6) at 4000 rpm for 30 s and then sintered at 500 °C for 30 min. Finally, the mesoporous TiO_2 films were immersed in 40 mM $TiCl_4$ aqueous solutions for 30 min at 70 °C and washed with deionized water and ethanol, followed by annealing at 500 °C for 30 min in air. The PVC was dissolved in chlorobenzene to obtain 0.5, 1.0 and 1.5 mg ml^{-1} concentration solution, respectively. Then PVC solutions were respectively spin coated onto the TiO_2 mesoporous layer at 1000 rpm for 10s to form the ultrathin PVC modified layer. A perovskite solution (1.25 mol L^{-1}) was prepared by blending MAI (0.2963 g) and PbI_2 (0.8678 g) powders in γ-butyrolactone (GBL) (1.05 mL) and dimethyl sulphoxide (DMSO) (0.45 mL). The perovskite layers were spin-coated onto TiO_2 mesoporous layer with one-step spin-coating procedure at 4000 rpm 50s assisted with solvent modified engineering. Anhydrous ether was dripped onto the perovskite layer before spin-coating end time of 30s. Then, the perovskite samples were annealed at 100 °C for 30 min. 72.3 mg of Spiro-OMeTAD and 28.8 μL TBP powers, and 17.5 μL Li-TFSI in acetonitrile (520 mg ml^{-1}) were dissolved in 1 mL chlorobenzene to form Spiro-OMeTAD solution. The Spiro-OMeTAD layer was spin-coated onto the perovskite layer at 4000 rpm for 30s. Finally, a 100 nm AgAl electrode with an active area of 0.1 cm^2 was thermally evaporated onto Spiro-OMeTAD layer at the base pressure of 5 × 10^{-4} Pa.

2.3. Characterization

X-ray diffraction (XRD) spectra were measured using a Bruker New D8 Advance with a Cu-Kα radiation source (λ: 1.5406 A) at 40 kV and 300 mA (12 kW). SEM images were performed by field-emission scanning electron microscopy (Hitachi S-4800). The photoluminescence (PL) spectra were measured with a fluorescence spectrophotometer (FluoroMax-4, HORIBA Jobin–Yvon). The transmission and absorption spectra of samples were measured using a UV–Vis spectrophotometer (U-3900, Hitachi). The current density–voltage (J–V) curves were measured using a Keithley model 2440 source meter and a Newport solar simulator system with AM1.5G and 100 mW cm^{-2} illumination calibrated by a standard silicon reference cell (Newport Oriel Instruments 91150V) in the air. The incident photon to current conversion efficiency (IPCE) spectra were measured in the air using a Newport Optical Power Meter 2936-R (74125, Oriel, USA). The grazing-incidence wide-angle X-ray scattering (GIWAXS) was performed at BL16B1 beam line of Shanghai Synchrotron Radiation Facility. The wavelength of GIWAXS was 0.124 nm and sample-to-detector distance was 220 mm. The incidence light angle was 0.15° and using MAR165CCD detector to collect the scattering signals.

3. Results and discussion

Fig. 1 shows SEM images of $MAPbI_3$ films onto TiO_2 layers without and with PVC modification. As shown in Fig. 1(b), the grain sizes of perovskite films with PVC modified TiO_2 layer are about 500–600 nm, which are obviously larger than that (200–400 nm) of perovskite layer onto the pure TiO_2 layers, as shown in Fig. 1(a), indicating that PVC modified the interface of TiO_2/perovskite layers help to improve the crystallization of perovskite layer. Furthermore, the perovskite layers with PVC modification show more compact films with less pin-holes, as shown in Fig. 1(c–d), which are expected to greatly reduce the leakage current of PSCs [30–34]. The better compact and crystallinity perovskite layer is related to the enhanced interface properties and the interaction between Pb^{2+} of $MAPbI_3$ and N atom in PVC [27]. The thickness of TiO_2,

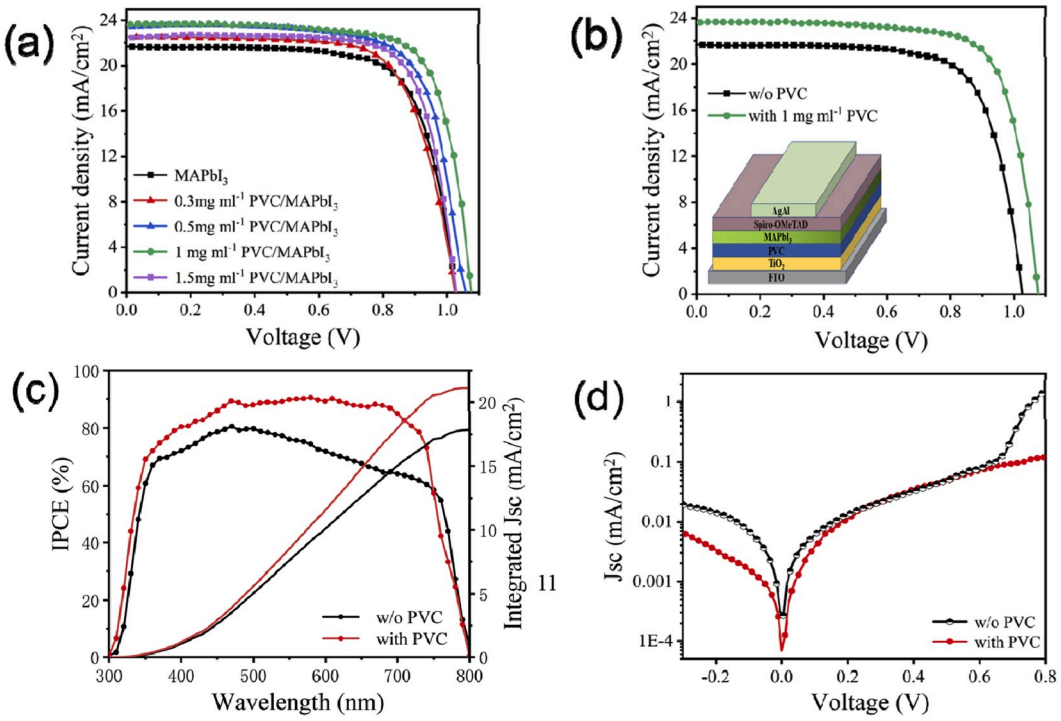

Fig. 3. (a) J-V curves of PSCs modified with PVC of different concentration. (b) J-V curves of PSCs without and with PVC modification of 1 mg ml^{-1}. (c) IPCE spectra and corresponding integrated current densities of PSCs with pristine TiO_2 and PVC modified TiO_2 layer. (d) Dark J-V curves of PSCs based on pristine TiO_2 and PVC modified TiO_2 layer.

Table 1
Summary of parameters of PSCs with different PVC concentration. The average values were calculated from 12 devices for each condition from different batches.

Devices	V_{OC} (V)	J_{SC} (mA cm^{-2})	FF (%)	PCE (%)	R_S (Ω cm^2)	R_{SH} (Ω cm^2)
reference device	1.03 ± 0.02	21.62 ± 1.02	72.56 ± 3.25	16.09 ± 1.56	62	6547
0.3 mg ml^{-1} PVC	1.02 ± 0.01	22.49 ± 0.71	69.58 ± 2.61	16.44 ± 1.32	46	12065
0.5 mg ml^{-1} PVC	1.06 ± 0.01	23.35 ± 0.35	73.02 ± 1.62	18.01 ± 0.87	56	14082
1 mg ml^{-1} PVC	1.07 ± 0.01	23.65 ± 0.27	74.75 ± 1.07	19.02 ± 0.52	38	17476
1.5 mg ml^{-1} PVC	1.03 ± 0.02	22.51 ± 0.46	75.3 ± 1.92	17.46 ± 1.73	40	13654

$MAPbI_3$ and Spiro-OMeTAD layers were clearly observed from the cross-section SEM images of Fig. 1(e–f). However, the ultrathin PVC modified layer cannot be distinguished from the cross-section SEM image due to the limited SEM resolution, indicating that the thickness of PVC modified layer is at the most several nanometers. The ultrathin PVC modified layer helps to tunnel electrons from perovskite to TiO_2 layers.

GIWAXS measurements can further understand the crystallization of perovskite layer. The two-dimensional GIWAXS images of perovskite films without and with PVC modification are shown in Fig. 2(a–b). Fig. 2 (c) shows the corresponding in-plane integrated lines along the q_{xy} direction. The Bragg rings in the film plane at q = 1.01 Å^{-1}, 2.01 Å^{-1} and 2.25 Å^{-1} are respectively corresponding to (110), (202) and (220) planes of perovskite film [31,32]. The intensity of peak belonging to (110) plane of PVC modified perovskite film became obviously stronger than that of the reference perovskite layer, indicating that PVC modified TiO_2/perovskite interface can improve the crystallization of perovskite layer [33]. Fig. 2(d) shows XRD spectra of perovskite films on TiO_2 layer modified with and without PVC. The characteristic diffraction peaks at 14.16°,28.48° and 31.92° are corresponding to (110), (220) and (310) planes of perovskite layers. The relatively strong (110) peak of the perovskite film with PVC modification further suggests that PVC modification help to improve the crystallization and grain sizes of perovskite film, which is consistent with the observed GIWAXS patterns and SEM images.

To demonstrate the effects of PVC modified TiO_2 film as a novel electron transport layer, the serial PSCs modified with different PVC concentration are investigated. The J−V curves of PSCs modified with different concentration PVC solution under AM 1.5 G irradiation at 100 mW cm^{-2} are shown in Fig. 3(a). The relative parameters of different kinds of PSCs are listed in Table 1. The short-circuit photocurrent density (J_{sc}), open circuit voltage (V_{oc}) and fill factor (FF) of PSCs with PVC modification are obviously higher than that of the pristine PSCs. Furthermore, PSCs modified with PVC concentration of 1 mg ml^{-1} got the best PCE.

Fig. 3(b) shows J-V curves of typical PSCs with and w/o PVC modification of 1 mg ml^{-1}. The pristine PSC showed 16.09% of PCE with J_{sc} = 21.62 mA/cm^2, V_{oc} = 1.03 V, FF = 72.6%. PSCs with PVC modification got 19.02% of PCE with J_{sc} = 23.65 mA/cm^2, V_{oc} = 1.075 V, FF = 74.6%, which is obviously higher than that of reference PSCs. Fig. 3(c) shows IPCE curves of the corresponding PSCs. The IPCE values of PSC with PVC modification is obviously higher than that of the pristine one especially in the wavelength range of 500–750 nm.The integrated J_{sc} values of PSCs were lower than the values obtained from J-V measurements is probably attributed to the defects of cells and part deviation of IPCE measurement [35]. The reduced dark current densities of PSCs with PVC modification was further observed, as shown in Fig. 3(d). These results indicated that PSCs modified with PVC can reduce carrier recombination and improve the interface contact properties, which help to improve J_{sc} and FF of PSCs [35,36].

The perovskite layer is easily deteriorated under moisture, heat and UV exposure due to its inferior stability, which became an important obstacle to realize its industry application. As shown in Fig. 4(a), the reference PSCs without encapsulation were quickly decayed and

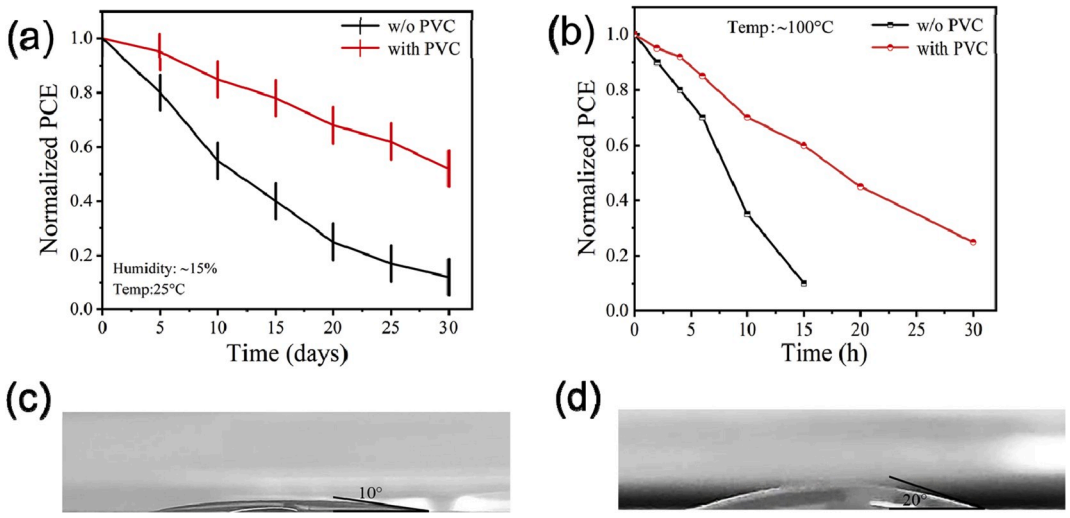

Fig. 4. (a) Stability of unencapsulated PSCs with aging time under RH of 15% in the ambient condition. (b) Normalized PCE values of PSCs without and with PVC modification as a function of annealed time at 100 °C in N_2-filled glove box. Contact angles of TiO_2 without (c) and with (d) PVC modification.

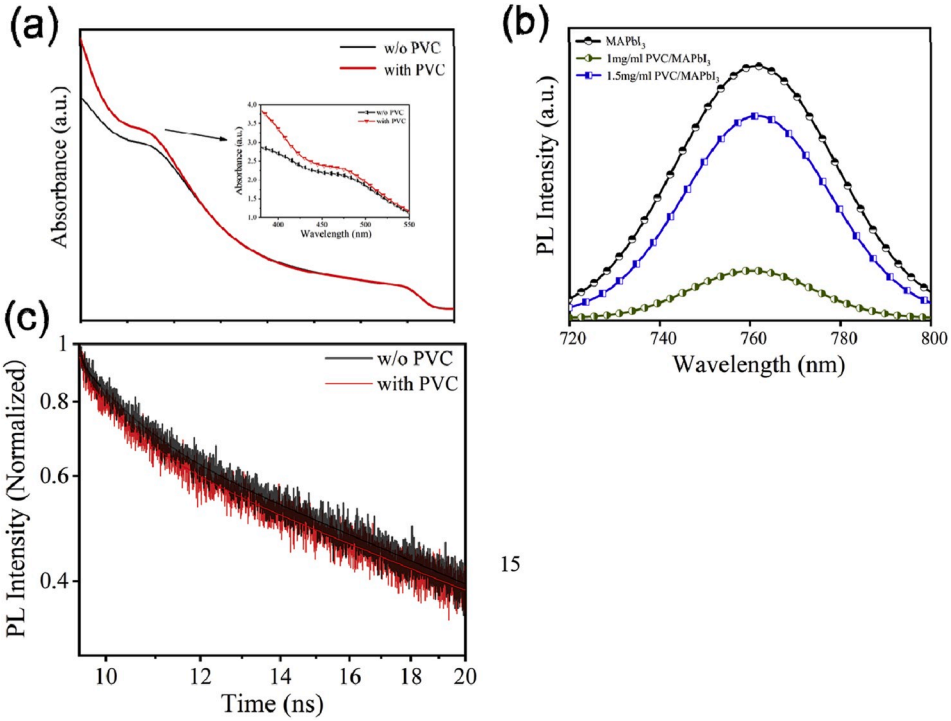

Fig. 5. (a) Absorption spectra of perovskite films on TiO_2 modified without and with PVC modification (PVC concentration of 1 mg ml^{-1}) (b) PL spectra of perovskite films onto TiO_2 modified without and with PVC. (c) Time-resolved PL curves of perovskite films without and with PVC modification.

remained only 20% of the initial PCE values aging for 30 days at relative humidity (RH) of 15%. Correspondingly, PSCs modified with PVC still remained about 55% of the initial PCE values aging for 30 days, indicating that PSCs modified with PVC show better moisture resistance. Furthermore, $MAPbI_3$ layers with and without PVC modification were tested under a high temperature of 100 °C in a N_2-filled glove box before further spin-coating Spiro-OMeTAD hole transport layer. As shown in Fig. 4(b), PSCs with PVC modification were decreased to 70% of the original PCEs after heating for 10 h at 100 °C, which are obviously superior to that (30%) of the original PCEs of the reference PSCs, indicating that PSCs with PVC modification shows superior thermal stability. The enhanced stability of PSCs with PVC modified TiO_2/perovskite interface is possibly attributed to better crystallization, interface passivation and the hydrophobicityinterface due to PVC interaction with TiO_2 and perovskite layers and its hydrophobicity [27,29,37]. The hydrophobicityproperty of PVC modified TiO_2/perovskite interface can be supported from the contact angles of TiO_2 layers without (10°) and with (20°) PVC modification, as shown in Fig. 4(c-d) [34]. The increased contact angle for PVC modified TiO_2 layer help to reduce the perovskite nuclei density and improve the crystallinity of perovskite layer [26].

To investigate the mechanism of enhanced PSCs with PVC modified mp-TiO_2 layer, optical characteristics of the perovskite layers and the electrochemical impedance spectra of PSCs were further measured. Fig. 5(a) shows the absorption spectra of perovskite films onto TiO_2 modified with and without PVC. The perovskite film modified with PVC

Table 2
Summarized fitting parameters taken from TRPL curves with three exponential decay functions.

Samples	A_1	τ_1 (ns)	A_2	τ_2 (ns)	A_3	τ_2 (ns)	$\tau_{amp\ avg}$ (ns)
TiO_2/PVC/ Perovskite	2.778	0.096	42.8	9.409	20.19	1.118	6.46
TiO_2/ Perovskite	2.13	0.070	47.1	10.638	19.66	1.213[7]	7.62

show stronger absorption, especially in the wavelength range of 400–520 nm, which further support better crystallinity of perovskite film [38,39]. Fig. 5(b) shows the PL intensities of perovskite films onto TiO_2 modified with and without PVC layer. Steady-state photoluminescence (PL) intensity of perovskite film is related to carrier recombination, carrier transport and extraction abilities at the interfaces between perovskite and carrier transport layers [34,38]. The quenched PL intensity for perovskite films with PVC modification indicate that carriers can be quickly transported and extracted to TiO_2 from perovskite layers [38]. Furthermore, PL intensity of perovskite layer modified with 1 mg ml^{-1} PVC concentration is obviously lower than that of perovskite modified with 1.5 mg ml^{-1} PVC concentration, indicating that carrier transportation and extraction abilities are related to the tunneling thickness of PVC modified layer. Although the ultrathin PVC modified layer cannot be distinguished from the cross-section SEM image of Fig. 1(f), the optimized PVC tunneling thickness is still important to improve transport and extraction of electrons from perovskite to TiO_2 layers, which is consistent with the obtained best PCEs of PSCs with 1 mg ml^{-1} PVC modification.

Time-resolved PL (TRPL) decay curves of PSCs without and with PVC modification are shown in Fig. 5(c). The fitted parameters of TRPL curves are summarized in Table 2. The TRPL spectra can provide a direct insight into the photo-physical properties of PSCs, including the charge accumulation at ETL/perovskite interface and the charge transfer or charge separation/injection behaviors [37,40]. The TRPL curves were fitted by a tri-exponential function as:

PL intensity = $A_1 \exp(-t/\tau_1) + A_2 \exp(-t/\tau_2) + A_3 \exp(-t/\tau_3)$. where A_1, A_2, and A_3 are time independent coefficients of amplitude fraction for each decay component, and τ_1, τ_2 and τ_3 are decay time of fast, intermediate, and slow components, respectively [37]. The amplitude average decay time ($\tau_{amp\ avg} = \frac{\sum iAi\tau i}{\sum iAi}$) of perovskite layer with and without PVC modification were 6.46 ns and 7.62 ns, respectively. The quickly decay lifetime and lower PL intensity of perovskite layer modified with PVC indicate that the ultrathin PVC modified layer can promote electrons tunnel from perovskite to TiO_2 layers and improve electrons transport and extraction, leading to better PCEs for PVC modified PSCs [41].

Fig. 6(a) presents the electrochemical impedance spectra measured in the frequency range from 0.1-10^6 Hz at a forward bias of 1 V in the dark situation. A clear semicircle can be distinguished in the intermediate-frequency region for all PSCs, which is related to charge recombination at related interfaces of PSCs [42]. The recombination resistance (Rct) of the pristine PSCs is larger than that PSCs modified with PVC, indicating that the incorporation of PVC modified layer can effectively reduce carrier recombination due to interface passivation and blocking holes transport into the TiO_2/perovskite interface [26]. Fig. 6(b) shows the dependence of V_{oc} on the light intensity. V_{oc} is function temperature (T) and J_{sc} of photovoltaic cell, described as, $V_{oc}=(nk_BTq^{-1})\ln(J_{sc}/J_0+1)$, where n is ideality factor, k_B is the

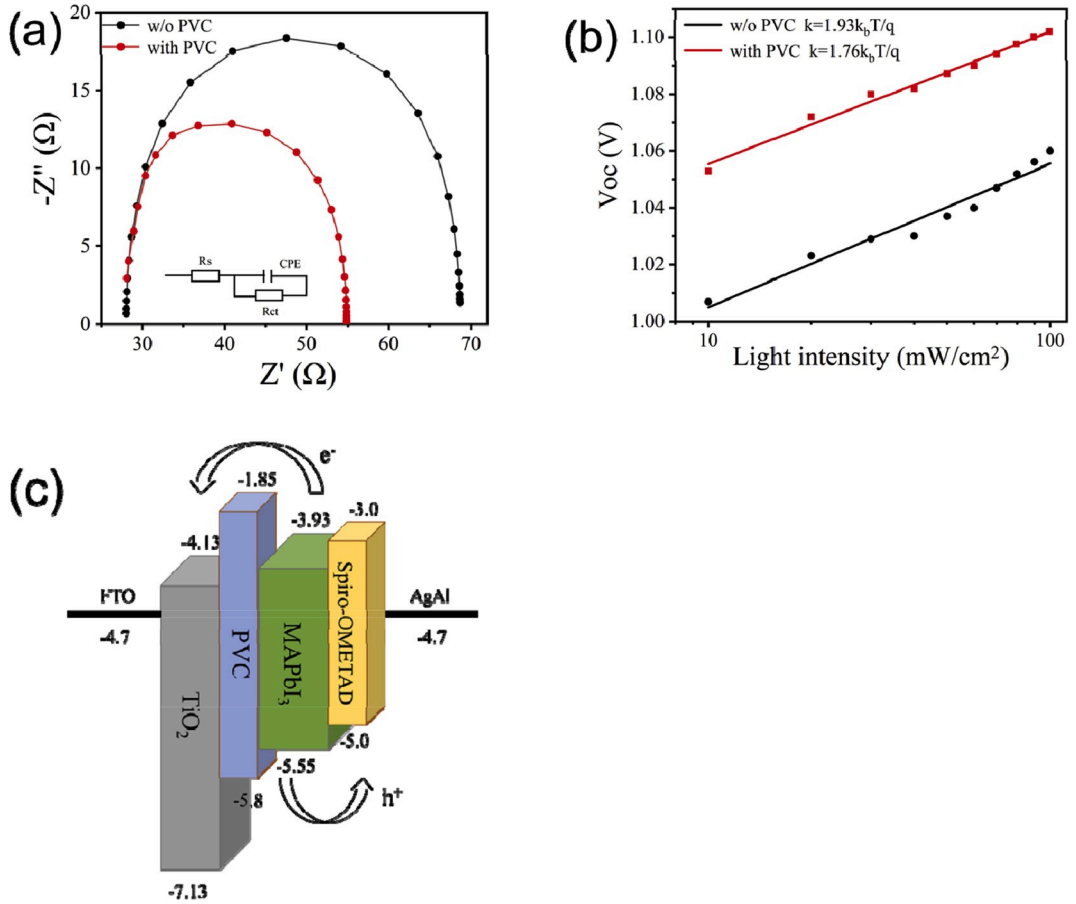

Fig. 6. (a) Nyquist plots of PSCs with and without PVC modification. (b) V_{oc} as a function of light density for PSCs. (c) Energy diagram of each layer of PSCs.

Boltzmann constant, T is absolute temperature, and q is elementary charge, J_0 is saturated current density (in the dark). Because $J_{sc} \gg J_0$ and $J_{sc} \propto$ light intensity, V_{oc} dependence on the natural logarithm of light intensity thus gives a slope of nk_BTq^{-1}. The simulated slopes of 1.93 k_BTq^{-1}, 1.76k_BTq^{-1} were obtained from w/o and with PVC modification. Hence the reduced ideality factor of PSCs modified with PVC compared to the reference PSCs, further demonstrating that PVC can reduce carrier recombination due to passivation effects and blocking hole carriers [43,44].

Fig. 6(c) shows the energy diagram of each layer of PSCs. The Highest Occupied Molecular Orbital (HOMO) and Lowest Unoccupied Molecular Orbital (LUMO) energy levels of PVC layer are about 5.8eV and 1.85eV, respectively [45]. The ultrathin PVC modified layer interacted with perovskite layer may reduce HOMO energy levels and still retain the deeper HOMO level of PVC compared to perovskite layer [27], which can block holes transport into the TiO_2/perovskite interface and reduce carrier accumulation and recombination at TiO_2/perovskite interface [26,34]. In the meantime, the electrons of perovskite layer can be easily tunneled from perovskite to TiO_2 layers due to the ultrathin PVC modified layer. The interaction between N atom of PVC and Pb^{2+} and I^- of the perovskite layer and the hydroxy proton of TiO_2 surface [26–29] can passivate TiO_2/perovskite interface and improve the crystallinity of perovskite layer, which can increase tunneling electric field of interface and improve the tunneling effect of interface [27]. Therefore, PVC integrated effects can effectively improve the PCEs of PSCs and stability.

4. Conclusions

In summary, the mesoporous PSCs with the FTO/TiO_2/PVC/$MAPbI_3$/spiro-OMeTAD/AgAl have been investigated. The P-type polymer material named PVC(9-vinylcarbazole) was selected to modify perovskite/TiO_2 interface. PSCs with PVC modified TiO_2 layer achieved average PCE of 19.02%, which is much higher than that of reference cells. The PVC modified PSCs remained 55% of the original PCE values aging for 30 days at RH 15% under ambient air, indicating that PSCs with PVC modification show better moisture resistance. In the meanwhile, the perovskite layer modified with PVC show better thermal stability. The enhanced performance of PSCs with PVC modified TiO_2 layer is attributed to the improved crystallinity of perovskite layer with less pinholes, passivating the interface and inhibiting hole carriers to transport into perovskite/TiO_2 interface. Therefore, using P-type organic semiconducting polymer with wide band-gap have obviously advantages for reducing hole accumulation of interface and inhibiting hole carriers to transport into the interface of perovskite/TiO_2 electron transport layers, indicating that using p-type organic materials modified TiO_2 electron transport layer is an effective method to improve the performance of PSCs.

Declaration of competing interest

The authors declare no conflict of interest.

Acknowledgement

This work is supported by the Natural Science Foundation of Shanghai (Nos. 18ZR1411000 and 18ZR1411900), Provincial Natural Science Foundation of Anhui (1908085ME120) and Innovative Research Team of Anhui Provincial Education Department (2016SCXPTTD). We also thank the Shanghai Synchrotron Radiation Facility (SSRF) for providing the BL16B1 beam line for collecting synchrotron GIWAXS data.

References

[1] National Renewable Energy Laboratory (NREL), Research cell efficiency records. https://www.nrel.gov/pv/cell-efficiency.html. (Accessed 7 May 2019).
[2] H. Liu, Z. Huang, S. Wei, L. Zheng, L. Xiao, Q. Gong, Nano-structured electron transporting materials for perovskite solar cells, Nanoscale 8 (2016) 6209–6221.
[3] Z. Zhu, J. Ma, Z. Wang, C. Mu, Z. Fan, L. Du, Y. Bai, L. Fan, H. Yan, D.L. Phillips, S. Yang, Efficiency enhancement of perovskite solar cells through fast electron extraction: the role of graphene quantum dots, J. Am. Chem. Soc. 136 (2014) 3760–3763.
[4] M. Chen, R.-H. Zha, Z.-Y. Yuan, Q.-S. Jing, Z.-Y. Huang, X.-K. Yang, S.-M. Yang, X.-H. Zhao, D.-L. Xu, G.-D. Zou, Boron and phosphorus co-doped carbon counter electrode for efficient hole-conductor-free perovskite solar cell, Chem. Eng. J. 313 (2017) 791–800.
[5] M. Saliba, T. Matsui, J.Y. Seo, K. Domanski, J.P. Correa-Baena, M.K. Nazeeruddin, S.M. Zakeeruddin, W. Tress, A. Abate, A. Hagfeldt, M. Gratzel, Cesium-containing triple cation perovskite solar cells: improved stability, reproducibility and high efficiency, Energy Environ. Sci. 9 (2016) 1989–1997.
[6] D.-Y. Son, J.-W. Lee, Y.J. Choi, I.-H. Jang, S. Lee, P.J. Yoo, H. Shin, N. Ahn, M. Choi, D. Kim, N.-G. Park, Self-formed grain boundary healing layer for highly efficient CH3NH3PbI3 perovskite solar cells, Nat. Energy 1 (2016) 16081.
[7] X. Huang, Z. Hu, J. Xu, P. Wang, J. Zhang, Y. Zhu, Low-temperature processed ultrathin TiO2 for efficient planar heterojunction perovskite solar cells, Electrochim. Acta 231 (2017) 77–84.
[8] D. Liu, S. Li, P. Zhang, Y. Wang, R. Zhang, H. Sarvari, F. Wang, J. Wu, Z. Wang, Z. D. Chen, Efficient planar heterojunction perovskite solar cells with Li-doped compact TiO 2 layer, Nano Energy 31 (2017) 462–468.
[9] D. Liu, T.L. Kelly, Perovskite solar cells with a planar heterojunction structure prepared using room-temperature solution processing techniques, Nat. Photon. 8 (2013) 133–138.
[10] M.H. Kumar, N. Yantara, S. Dharani, M. Graetzel, S. Mhaisalkar, P.P. Boix, N. Mathews, Flexible, low-temperature, solution processed ZnO-based perovskite solid state solar cells, Chem. Commun. (Camb) 49 (2013) 11089–11091.
[11] H.-S. Rao, B.-X. Chen, W.-G. Li, Y.-F. Xu, H.-Y. Chen, D.-B. Kuang, C.-Y. Su, Improving the extraction of photogenerated electrons with SnO2Nanocolloids for efficient planar perovskite solar cells, Adv. Funct. Mater. 25 (2015) 7200–7207.
[12] C. Gao, S. Yuan, B. Cao, J. Yu, SnO 2 nanotube arrays grown via an in situ template-etching strategy for effective and stable perovskite solar cells, Chem. Eng. J. 325 (2017) 378–385.
[13] F. Giordano, A. Abate, J.P. Correa Baena, M. Saliba, T. Matsui, S.H. Im, S. M. Zakeeruddin, M.K. Nazeeruddin, A. Hagfeldt, M. Graetzel, Enhanced electronic properties in mesoporous TiO2 via lithium doping for high-efficiency perovskite solar cells, Nat. Commun. 7 (2016) 10379.
[14] X. Hou, T. Xuan, H. Sun, X. Chen, H. Li, L. Pan, High-performance perovskite solar cells by incorporating a ZnGa2O4:Eu3+ nanophosphor in the mesoporous TiO2 layer, Sol. Energy Mater. Sol. Cell. 149 (2016) 121–127.
[15] C. Zhang, Y. Luo, X. Chen, Y. Chen, Z. Sun, S. Huang, Effective improvement of the photovoltaic performance of carbon-based perovskite solar cells by additional solvents, Nano-Micro Lett. 8 (2016) 347–357.
[16] D. Bi, W. Tress, M.I. Dar, P. Gao, J. Luo, C. Renevier, K. Schenk, A. Abate, F. Giordano, J.-P.C. Baena, J.-D. Decoppet, S.M. Zakeeruddin, M.K. Nazeeruddin, M. Gratzel, A. Hagfeldt, Efficient luminescent solar cells based on tailored mixed-cation perovskites, Sci. Adv. 2 (2016), e1501170.
[17] Y. Huang, J. Zhu, Y. Ding, S. Chen, C. Zhang, S. Dai, TiO2 sub-microsphere film as scaffold layer for efficient perovskite solar cells, ACS Appl. Mater. Interfaces 8 (2016) 8162–8167.
[18] H. Tan, A. Jain, O. Voznyy, X. Lan, F.P.G. de Arquer, J.Z. Fan, R. Quintero-Bermudez, M. Yuan, B. Zhang, Y. Zhao, F. Fan, P. Li, L.N. Quan, Y. Zhao, Z.-H. Lu, Z. Yang, S. Hoogland, E.H. Sargent, Efficient and stable solution-processed planar perovskite solar cells via contact passivation, Science 355 (2017) 722–726.
[19] H. Zhang, J. Shi, X. Xu, L. Zhu, Y. Luo, D. Li, Q. Meng, Mg-doped TiO2 boosts the efficiency of planar perovskite solar cells to exceed 19%, J. Mater. Chem. 4 (2016) 15383–15389.
[20] X. Zhang, Z. Bao, X. Tao, H. Sun, W. Chen, X. Zhou, Sn-doped TiO2nanorod arrays and application in perovskite solar cells, RSC Adv. 4 (2014) 64001–64005.
[21] B.J. Kim, M.c. Kim, D.G. Lee, G. Lee, G.J. Bang, J.B. Jeon, M. Choi, H.S. Jung, Interface design of hybrid electron extraction layer for relieving hysteresis and retarding charge recombination in perovskite solar cells, Adv. Mater. Interfaces 5 (2018) 1800993.
[22] Y. Yue, T. Umeyama, Y. Kohara, H. Kashio, M. Itoh, S. Ito, E. Sivaniah, H. Imahori, Polymer-assisted construction of mesoporous TiO2 layers for improving perovskite solar cell performance, J. Phys. Chem. C 119 (2015) 22847–22854.
[23] O. Ostroverkhova, W.E. Moerner, Organic photorefractives: mechanisms, materials, and applications, Chem. Rev. 104 (2004) 3267–3314.
[24] J.L. Maldonado, Y. Ponce-de-León, G. Ramos-Ortíz, M. Rodríguez, M.A. Meneses-Nava, O. Barbosa-García, R. Santillán, N. Farfán, High diffraction efficiency at low electric field in photorefractive polymers doped with arylimine chromophores, J. Phys. Appl. Phys. 42 (2009), 075102.
[25] A. Álvarez-Fernández, J.-L. Maldonado, E. Pérez-Gutiérrez, M. Rodríguez, G. Ramos-Ortíz, O. Barbosa-García, M.-A. Meneses-Nava, M.G. Zolotukhin, Performance and stability of PTB7:PC71BM based polymer solar cells, with ECZ and/or PVK dopants, under the application of an external electric field, J. Mater. Sci. Mater. Electron. 27 (2016) 6271–6281.
[26] Y. Liu, J. Duan, J. Zhang, S. Huang, W. Ou-Yang, Q. Bao, Z. Sun, X. Chen, High efficiency and stability of inverted perovskite solar cells using phenethyl

ammonium iodide-modified interface of NiOx and perovskite layers, ACS Appl. Mater. Interfaces 12 (2020) 771–779.
[27] J. Zhang, W. Mao, J. Duan, S. Huang, Z. Zhang, W. Ou-Yang, X. Zhang, Z. Sun, X. Chen, Enhanced efficiency and thermal stability of perovskite solar cells using poly(9-vinylcarbazole) modified perovskite/PCBM interface, Electrochim. Acta 318 (2019) 384–391.
[28] J. Zhang, W. Liang, W. Yu, S. Yu, Y. Wu, X. Guo, S. Liu, C. Li, A two-stage annealing strategy for crystallization control of CH3NH3PbI3 films toward highly reproducible perovskite solar cells, Small 14 (2018) 1800181.
[29] Y. Ooyama, S. Inoue, R. Asada, G. Ito, K. Kushimoto, K. Komaguchi, I. Imae, Y. Harima, Dye-sensitized solar cells based on a novel fluorescent dye with a pyridine ring and a pyridinium dye with the pyridinium ring forming strong interactions with nanocrystalline TiO2 films, Eur. J. Org Chem. (2010) 92–100, 2010.
[30] K.A. Bush, N. Rolston, A. Gold-Parker, S. Manzoor, J. Hausele, Z.J. Yu, J.A. Raiford, R. Cheacharoen, Z.C. Holman, M.F. Toney, R.H. Dauskardt, M.D. McGehee, Controlling thin-film stress and wrinkling during perovskite film formation, ACS Energy Lett. 3 (2018) 1225–1232.
[31] H. Lai, B. Kan, T. Liu, N. Zheng, Z. Xie, T. Zhou, X. Wan, X. Zhang, Y. Liu, Y. Chen, Two-dimensional ruddlesden-Popper perovskite with nanorod-like morphology for solar cells with efficiency exceeding 15%, J. Am. Chem. Soc. 140 (2018) 11639–11646.
[32] C.M.M. Soe, W. Nie, C.C. Stoumpos, H. Tsai, J.-C. Blancon, F. Liu, J. Even, T. J. Marks, A.D. Mohite, M.G. Kanatzidis, Understanding film formation morphology and orientation in high member 2D ruddlesden-Popper perovskites for high-efficiency solar cells, Adv. Energy Mater. 8 (2018) 1700979.
[33] Y. Cai, Z. Zhang, Y. Zhou, H. Liu, Q. Qin, X. Lu, X. Gao, L. Shui, S. Wu, J. Liu, Enhancing the efficiency of low-temperature planar perovskite solar cells by modifying the interface between perovskite and hole transport layer with polymers, Electrochim. Acta 261 (2018) 445–453.
[34] X. Hou, S. Huang, O.-Y. Wei, L. Pan, Z. Sun, X. Chen, Constructing efficient and stable perovskite solar cells via interconnecting perovskite grains, ACS Appl. Mater. Interfaces 9 (2017) 35200–35208.
[35] Z. Jiang, X. Chen, X. Lin, X. Jia, J. Wang, L. Pan, S. Huang, F. Zhu, Z. Sun, Amazing stable open-circuit voltage in perovskite solar cells using AgAl alloy electrode, Sol. Energy Mater. Sol. Cell. 146 (2016) 35–43.
[36] B. Li, C. Zheng, H. Liu, J. Zhu, H. Zhang, D. Gao, W. Huang, Large planar pi-conjugated porphyrin for interfacial engineering in p-i-n perovskite solar cells, ACS Appl. Mater. Interfaces 8 (2016) 27438–27443.
[37] X. Hou, J. Zhou, S. Huang, W. Ou-Yang, L. Pan, X. Chen, Efficient quasi-mesoscopic perovskite solar cells using Li-doped hierarchical TiO2 as scaffold of scattered distribution, Chem. Eng. J. 330 (2017) 947–955.
[38] M. Li, X. Yan, Z. Kang, X. Liao, Y. Li, X. Zheng, P. Lin, J. Meng, Y. Zhang, Enhanced efficiency and stability of perovskite solar cells via anti-solvent treatment in two-step deposition method, ACS Appl. Mater. Interfaces 9 (2017) 7224–7231.
[39] L. Gil-Escrig, C. Momblona, M.-G. La-Placa, P.P. Boix, M. Sessolo, H.J. Bolink, Vacuum deposited triple-cation mixed-halide perovskite solar cells, Adv. Energy Mater. 8 (2018) 1703506.
[40] J.H. Heo, H.J. Han, D. Kim, T.K. Ahn, S.H. Im, Hysteresis-less inverted CH3NH3PbI3 planar perovskite hybrid solar cells with 18.1% power conversion efficiency, Energy Environ. Sci. 8 (2015) 1602–1608.
[41] J.C. Yu, S. Badgujar, E.D. Jung, V.K. Singh, D.W. Kim, J. Gierschner, E. Lee, Y. S. Kim, S. Cho, M.S. Kwon, M.H. Song, Highly efficient and stable inverted perovskite solar cell obtained via treatment by semiconducting chemical additive, Adv. Mater. 31 (2019), e1805554.
[42] G. Garcia-Belmonte, A. Munar, E.M. Barea, J. Bisquert, I. Ugarte, R. Pacios, Charge carrier mobility and lifetime of organic bulk heterojunctions analyzed by impedance spectroscopy, Org. Electron. 9 (2008) 847–851.
[43] W. Tress, M. Yavari, K. Domanski, P. Yadav, B. Niesen, J.P. Correa Baena, A. Hagfeldt, M. Graetzel, Interpretation and evolution of open-circuit voltage, recombination, ideality factor and subgap defect states during reversible light-soaking and irreversible degradation of perovskite solar cells, Energy Environ. Sci. 11 (2018) 151–165.
[44] R. Fu, Y. Zhao, Q. Li, W. Zhou, D. Yu, Q. Zhao, Enhanced long-term stability of perovskite solar cells by 3-hydroxypyridine dipping, Chem. Commun. (Camb) 53 (2017) 1829–1831.
[45] J. Jeong, J. Lee, H. Lee, G. Hyun, S. Park, Y. Yi, S.W. Cho, H. Lee, Energy level alignment and hole injection property of poly(9-vinylcarbazole)/indium tin oxide interface, Chem. Phys. Lett. 706 (2018) 317–322.